Trends in Transplantation

Research Article ISSN: 1887-455X

Pilot Study on Cytothesis for rabbit ocular surface defects using peripheral blood autologous mononuclear cells

Hening Zhang[1#], Qijiong Li[2#], Min Zhang[1#], Minglei Zhao[1#], Mian Huang[3], Weihua Li[1], Wencong Wang[1], Bikun Xian[1], Ying Liu[1], Zhiquan Li[1], Yaojue Xie[1], Xiulan Zhang[1], Zhichong Wang[1*] and Bing Huang[1*]

[1]State Key Laboratory of Ophthalmology, Zhongshan Ophthalmic Center, Sun Yat-sen University, GuangZhou 510060, China

[2]Department of Hepatobiliary Oncology, Sun Yat-sen University Cancer, Center, 651 Dongfeng Rd. E., Guangzhou, Guangdong 510060, China

[3]Guangzhou Zoo, Guangzhou 510070, China

[#]Contributed equally

Abstract

At present, there is no effective treatment for severe ocular surface injury due to limbal stem cell deficiency. Stem cell transplantation offers hope for disease treatment, and the peripheral blood mononuclear cell fraction is a rich source of stem cells. In this study, rabbit autologous peripheral blood mononuclear cells were collected and combined with human amniotic membrane for repair of experimental ocular surface deficits. We observed good reparative effects, suggesting that autologous peripheral blood mononuclear cells are a promising stem cell source for the treatment of severe ocular surface injury.

Introduction

Many such studies have revealed that human (h)PBMCs are rich in pluripotent progenitor cells that can be differentiated into almost any triploblastic cell [1]. Compared to other adult pluripotent stem cells (e.g., from bone marrow and other tissues), PBSCs are easily obtained and easily separated [2]. Moreover, unlike embryonic stem cell (ESC)-based therapy, autologous transplantation of PBMCs does not require long-term use of immunosuppressive agents and involves no ethical limitations [3,4], while unlike induced pluripotent stem cells (iPSs), PBMCs carry little tumorigenic risk.

PBMCs have many possible applications for the treatment of eye diseases. For instance, Liu, *et al.* [5], Zhang, *et al.* [6], Peng, *et al.* [7], and Xian, *et al.* [8] transplanted PBMCs into the eyes of retinitis pigmentosa (RP) mice and observed migration of transplanted cells to all layers of the retina, indicating possible use for restoring retinal function. Limbal stem cells (LSCs) propagate and differentiate into corneal epithelial cells, allowing continuous renewal and dynamic stability of the corneal epithelium [9-12]. Further, the limbus isolates the cornea from the conjunctiva to prevent intrusion of conjunctival cells and neovascularization towards the cornea, thereby maintaining corneal transparency [13-17]. Limbal stem cell deficiency impairs this barrier function, resulting in conjunctival cell intrusion, neovascularization, and visual impairment [18].

Currently, LSCD are treated mainly by recovery of the LSC population using LSC transplantation [19-21], corneal epithelium transplantation [21], corneal transplantation [22], amniotic membrane transplantation [23-25], or induced differentiation of stem cell types to corneal limbal stem cells or corneal epithelial cells. Stem cells used for induce differentiation include induced pluripotent stem cells [26], mesenchymal stem cells [27,28], epidermal stem cells [29,30], and embryonic stem cells [18,31]. However, these methods have many weaknesses.

Adult stem cells isolated from PBMCs [1,6] are a promising alternative warranting further study. It is intended to provide a new ideology and approach for the treatment of severe ocular surface disorders caused by human limbal stem cell deficiency.

Material and methods

Experimental animals and grouping

Thirty healthy 4–5 month old New Zealand rabbits (15 male and 15 female) weighing 2.0–2.5 kg were randomly divided into three groups (1) Experimental group I (rPBMC); (2) Experimental group II (AM); (3) Negative control group (LSCD).

Experimental approach

Animal experimental ethics: All animal experiments were approved by the Laboratory Animal Ethics Committee of Zhongshan Ophthalmic Center, Sun Yat-Sen University (Approval Number: 2013-060). All animal procedures were performed in accordance with the Association for Research in Vision and Ophthalmology (ARVO) Statement for the Use of Animals in Ophthalmic and Vision Research.

Correspondence to: Bing Huang, State Key Laboratory of Ophthalmology, Zhongshan Ophthalmic Center, Sun Yat-sen University, GuangZhou 510060, China, E-mail: huangbing2000@hotmail.com

Zhichong Wang, State Key Laboratory of Ophthalmology, Zhongshan Ophthalmic Center, Sun Yat-sen University, GuangZhou 510060, China, E-mail: wzc001@hotmail.com

Key words: *peripheral blood stem cell, limbal stem cells deficiency, rabbit, neovascularization, transparency*

Received: June 01, 2020; **Accepted:** June 15, 2020; **Published:** June 18, 2020

Sourcing, processing, and preservation of human amniotic membranes: All HAMs were sourced from the discarded placentas of healthy women (with no HIV or CMV). Epithelial cells were scraped off and the remnants washed with sterile saline (or PBS), suspended in DMEM-F12, and maintained in a 37 °C.

Separation and tags of rabbit PBMCs: Autologous venous blood samples (20 mL) were extracted from the ear margins of experimental Group (rPBMC) rabbits. Mononuclear cells in blood were separated with rabbit PBMC separation medium (Hanyang Biology, Tianjin, China). CM-DiI-labeled and suspended in 1 ml of stem cell culture medium.

Graft Preparation: HAMs were cut into the grafts of about 1.5 × 1.5 cm and laid with the scraped epithelium face-up in 24-well plates. Autologous CM-DiI-labeled rPBMC suspensions were seeded on these HAM grafts and the cells separated from 1 rabbit were transplanted onto a HAM graft and cultured overnight at 37 °C in an incubator with 5% CO_2 and 100% humidity. The excess culture medium was removed and rinsed three times with PBS to remove non-adherent cells before transplantation the next day.

Modeling of rabbit ocular surface deficiency and Transplantation: Rabbit's corneal epithelium was scraped off using microsurgery forceps. Then, the tissues inside and outside of the corneal limbus with the width of 1–2 mm and the thickness of 100—150 μm were cut to build LSCD model. The prepared graft was placed over the corneal surface deficiency with the scraped epithelium/seeded side facing the lesion. In the negative control group (LSCD Group), the lesion was left untreated, while the AM group received unseeded HAM transplantation.

Observation of ocular surface signs: After transplantation, the rabbit operative eye was observed under a slit lamp once a week. Conjunctival congestion, secretion, corneal transparency, and neovascularization were observed and evaluated, the integrity of the corneal epithelium assessed using sodium fluorescein, and the eye photographed.

Confocal laser microscopy of living corneas: Changes in corneal epithelium were assessed under anesthesia in living cornea by confocal laser microscope (Heidelberg HRT3-RCM, Germany) on postoperative Weeks 1, 2, 3, and 4.

Histology: After completion of in situ examinations on Week 4 (Sections 2.7–2.8), rabbits were sacrificed and corneas isolated for hematoxylin and eosin (HE) staining, then observed and photographed under an optical microscope (Axio Imager A1 and AxioCAMMRc5; Carl Zeiss, Jena, Germany) for image processing and analysis (AxioVision; Carl Zeiss).

Immunocytochemistry and immunohistochemistry: Fresh rabbit PBMCs and some frozen corneal sections were stained for K3/K12, β-1 integrin, and CD45 protein to monitor changes in cell phenotype. The concentration of separated rPBMCs was diluted to 2–3 × 10^6/mL and cell smears prepared from 100-μL samples at 800 rpm with moderate acceleration for 2 min using a centrifugal smear machine (Thermo Shandon CYTOSPIN USA). Frozen corneal sections were fixed with 4% paraformaldehyde for 10 min and stained with mouse anti-rabbit K3/K12 (ab68260 abcam, UK), mouse anti-rabbit β-1 integrin (ab78502 abcam, UK), and (or) mouse anti-rabbit CD45 (AM02304PU-S, Acris Antibodies Inc USA). Immunolabeling was visualized with FITC-conjugated goat anti-mouse IgG (ab6785 abcam USA) and the nucleus was counterstained with 0.5 g/mL Hoechst33342 (Sigma, St. Louis, MI, USA). Observation, photography, and image analysis were conducted using a laser scanning confocal microscope (Carl Zeiss Meditec, Germany).

TUNEL staining (apoptosis): Some frozen sections (5-μm thick) were fixed in 4% paraformaldehyde and the cornea ruptured using 0.03% Triton-X for TUNEL staining with a FITC-conjugated TUNEL antibody kit (Beyotime, Jiangsu, China) according to the manufacturer's instructions. The nucleus counterstained with 0.5 g/mL Hoechst33342 (Sigma). Observation, photography, and image analysis were conducted using a laser scanning confocal microscope (Carl Zeiss Meditec, Germany).

Statistical analysis of corneal transparency and neovascularization: Corneal transparency and neovascularization were evaluated by Score Criteria for Ocular Surface Evaluation (Supplementary Table 1) [17,31]. Score results were compared among groups by ANOVA using SPSS Statistics Software (IBM). Quantit/ative results are expressed as mean ± standard deviation (Supplementary Tables 3 and 4) and change in mean over time (Figures 5 and 6).

Results

Morphology of rabbit PBMCs co-cultured with HAMs

HAMs were scraped of the epithelial layer and spread onto 24-well plates to form a basement membrane, which was clearly observed under light microscopy (Figure 1A). Rabbit PBMCs obtained from each animal of the experiment group (rPBMC Group, average (± SD) of $5.328\times10^7 \pm 1.071\times10^7$ cells; Supplementary Table 4) were small, round, and phase-bright in dispersed suspended culture (Fig. 1-B). Cell numbers increased substantially through overnight co-culture with HAMs (Figure 1C).

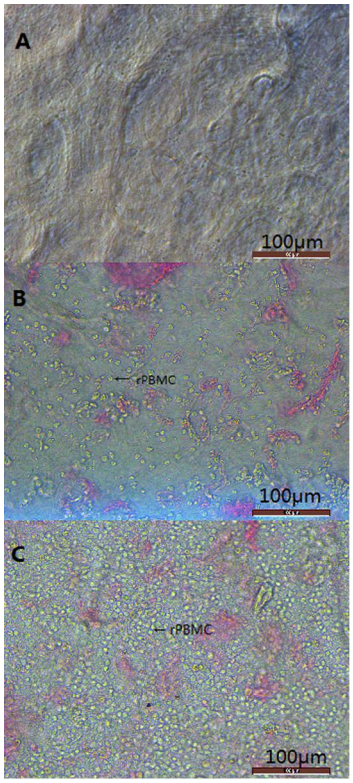

Figure 1. The images of amniotic membrane and rabbit

(A). Human amnion membrane were scraped epithelial layer.

(B). The suspension of peripheral blood mononuclear cells was added to the amniotic membrane, and a small amount of rPMBC was observed under the microscope.

(C). After 24 hours incubation, a large number of rPBMC clumps can be seen on the surface of the amniotic membrane.

Changes of ocular signs

The ocular surface of untreated rabbits showed no conjunctival congestion or secretion, high corneal transparency, and no neovascularization or fluorescein staining (indicating intact corneal epithelial layers) (Figure 2A and 2C). On the day of surgery, a few rabbit subjected to corneal surface lesion modeling exhibited conjunctival congestion but without secretions. Compared to normal eyes, lesioned eyes were significantly edematous, with reduced corneal transparency and extensive fluorescein staining indicative of a breached epithelium, but without neovascularization (Figure 2B and 2D). At all 4 postoperative observation times (1W, 2W, 3W, and 4W), the rPBMC Group exhibited the lowest levels of conjunctival congestion, secretion, corneal fluorescein staining, and neovascularization, and the highest corneal transparency, while the AM Group transplanted with HAMs but no PBMCs after lesioning showed only slight reparative effects compared to the model group receiving no transplantation (LSCD Group) (Figures 3 and 4, Supplementary Table 1 and 2). At postoperative 3W, operative eyes in rPBMC Group exhibited no secretion, a transparent cornea, and little neovascularization or fluorescein staining, while operative eyes in the AM Group still exhibited moderate (++) conjunctival congestion (although this groups also showed no secretions, relatively transparent corneas, and little neovascularization or corneal fluorescein staining). By 4W, operative eyes in the LSCD Group also showed no secretion, but there was still conjunctival congestion (++), opaque corneas and unobservable rear tissue, substantial neovascularization, and punctate surface fluorescein staining.

Statistical analysis of corneal transparency and neovascularization condition

Statistical analysis of corneal transparency: Based on observations of ocular signs (Figure 3, Supplementary Table 1 and 2) and evaluation scores (Supplementary Table 3), corneal transparency scores were obtained for each rabbit (Supplementary Table 5) and compared among groups by ANOVA (Figure 5A and 5C, Supplementary Table 6, Supplementary Figure 1). At all four postoperative observation times

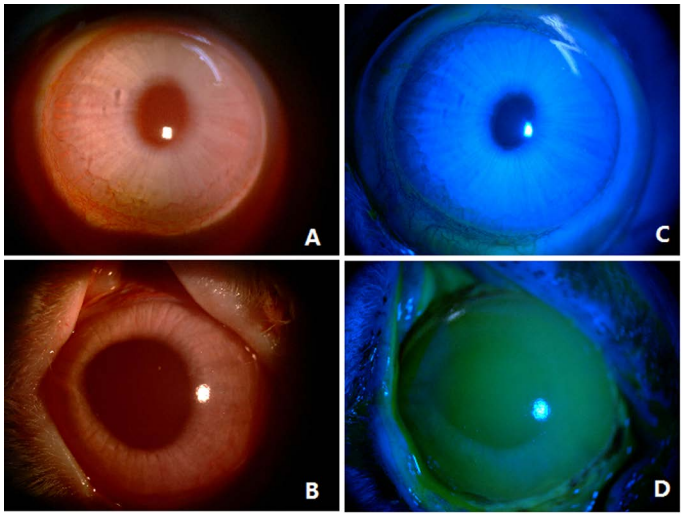

Figure 2. Rabbit normal and after modeling corneal manifestations

(A). Normal rabbit cornea

(B). Normal rabbit cornea without fluorescein staining

(C). Rabbit cornea after modeling

(D). Rabbit cornea after modeling full of corneal fluorescein staining

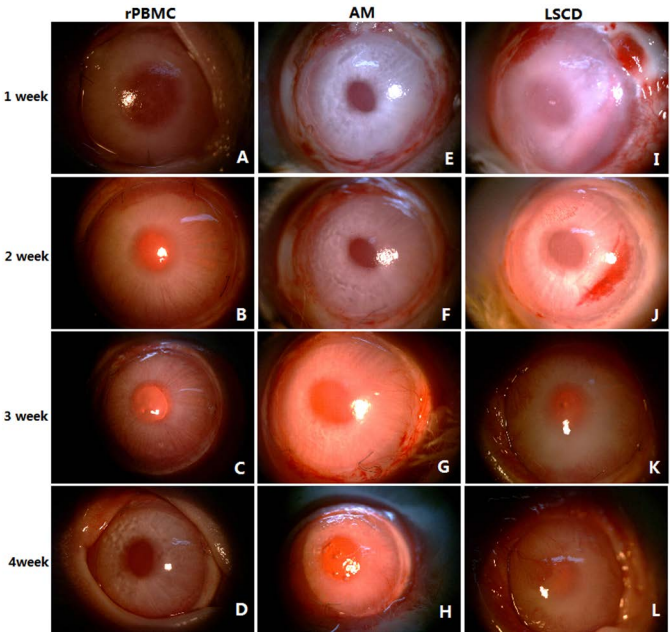

Figure 3. Clinic manifestations of rabbit cornea after operation

(A)-(D). Corneal changes in rPBMC group within four weeks after operation

(E)-(H). Corneal changes in AM group within four weeks after operation

(I)-(L). Corneal changes in LSCD group within four weeks after operation

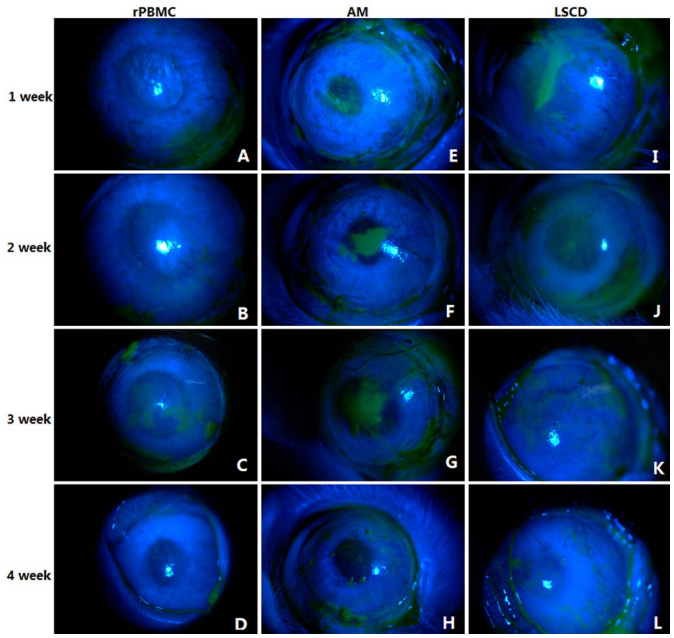

Figure 4. Fluorescein staining of rabbit cornea

(A)-(D). Fluorescein staining in rPBMC group within four weeks after operation

(E)-(H). Fluorescein staining in AM group within four weeks after operation

(I)-(L). Fluorescein staining in LSCD group within four weeks after operation

(1W, 2W, 3W, and 4W), corneal transparency differed significantly among the rPBMC, AM, LSCD Groups ($P<0.05$). The rPBMC Group had a significantly lower evaluation score at all four observation times than either the AM or LSCD Group, as well as the highest corneal transparency, while the AM Group had higher evaluation score and corneal transparency at all 4 observation times than the LSCD Group. Moreover, transparency scores (higher numbers indicating greater

opacity) in the LSCD group tended to increase over time, in contrast to rPBMC and AM groups.

Statistical analysis of corneal neovascularization condition: Based on the observation of ocular signs (Figure 3, Supplementary Table 1 and 2) and evaluation scores (Supplementary Table 3), corneal neovascularization score for each rabbit (Supplementary Table 7) was obtained and compared among groups by ANOVA (Figure 5B and 5D, Supplementary Table 8, Supplementary Figure 2). At all four postoperative observation times (1W, 2W, 3W, and 4W), corneal neovascularization differed significantly among groups ($P<0.05$), with significantly lower levels in the rPBMC Group than AM and LCD Groups ($P<0.05$). In turn, AM Group scores were lower than LSCD Group scores. Further, like transparency, neovascularization continued to increase with time in the LSCD group.

Corneal changes under confocal microscopy

Under confocal microscopy, the cell bodies of normal corneal epithelium were highly reflective, with centrally located and less reflective nuclei (Figure 6M-6P). In the rPBMC Group at postoperative 1W, corneal epithelial cells were clearly reflective but smaller than normal corneal epithelial cells (Figure 6I). At postoperative 2W, there was no increase in cell number, and cells exhibited clearly reflective nuclei and unclearly reflective somata (Figure 6J). At postoperative 3W and 4W, the number of cells was significantly increased and more densely arranged, with smaller somata and clearly reflective nuclei (Figure 6K and 6L). In the AM Group at postoperative 1W, no cells with high brightness and clear boundaries were observed in the field of view, but a few dark dot-like substances were observed (Figure 6E). At postoperative 2W, small cells with unclear nuclei were observed (Figure 6F). At postoperative 3W, the number of cells was not significantly increased and cells were still of smaller size with unclear nuclei (Figure 6G). Cell number still had not dramatically changed by postoperative 4W (Figure 7H). In the LSCD Group at postoperative 1W, numerous irregular bright reflective puncta without obvious cell morphology were observed under the microscope (Figure 6A). At postoperative 2W, the number of these reflections was reduced and no round cells could be observed under the microscope (Figure 6B). At postoperative 3W and 4W, a large amount of disorderly arranged fibrous tissues which were observed, with occasionally bright reflections. Again, no morphologically clear cells could be observed under the microscope (Figure 6C and 6D).

Histological changes

In normal cornea, 4–6 layers of epithelial cells were densely arrayed [Figure 7A (a)]. Similarly, limbal cells were also densely arrayed in multiple layers [Figure 7A (b)]. Immediately after surgery, the corneal epithelium and limbus were largely devoid of cells [Figure 7A (c) and 7A (d)].

At postoperative 4W, the rPBMC Group exhibited a growing corneal epithelium with 3–4 layers of epithelial cells in a dense array [Figure 7B (a)]. In contrast, the corneal epithelium of the AM Group grew poorly and remained disordered at W4. In addition, a few vacuolar cells could be observed and numerous inflammatory cells had infiltrated the basement layer of AM Group corneas [Figure 7B (b)]. In the LSCD Group, the epithelial layer also grew poorly. Epithelial cell layers were disordered, numerous vacuolar cells were observed, and a large number of inflammatory cells had infiltrated the basement layer [Figure 7B(c)]. Thus, repair of the corneal epithelium was markedly improved in the rPBMC Group compared to the AM and LSCD Groups

Immunofluorescence analysis of marker proteins

Rabbit PBMCs express CD45, but they do not express K3/K12, β-1 integrin (Supplementary Figure 3). Normal rabbit corneal epithelium expressed K3K/12 (Supplementary Figs. 4-5) and β-1 integrin (Supplementary Figure 5(1)).

At postoperative 1W, corneal epithelium of the rPBMC Group contained few K3/K12+ (Supplementary Fig. 4-1) or β-1 integrin+ cells (Supplementary Figure 5(1)). From postoperative 2W to 4W, the numbers of K3/12+ (Supplementary Figure 4(2)- 4(4)) and β-1 integrin+ cells (Supplementary Figure 5(2)-5(4)) gradually increased, indicating increased numbers of phenotypically normal endothelial cells.

Tunel staining of rabbit corneal epithelial cells

At postoperative 4W, only a few corneal epithelial cells in the rPBMC Group were TUNEL-positive (Supplementary Fig. 6-1), while

A

Group	WEEK 1	WEEK 2	WEEK 3	WEEK 4
LSCD	2.1±0.88	2.7±1.06	2.9±1.10	3.2±1.23
AM	1.7±0.95	2.1±0.99	2.3±0.95	2.5±0.97
rPBMC	0.9±0.57	0.7±0.48	0.9±0.32	1±0.47

B

Group	WEEK 1	WEEK 2	WEEK 3	WEEK 4
LSCD	2.5±0.97	3.2±0.92	3.4±0.97	3.3±0.95
AM	2.2±0.92	2.6±0.70	2.5±0.71	2.6±0.70
rPBMC	1.00±0.67	1.1±0.57	1.2±0.42	1.2±0.43

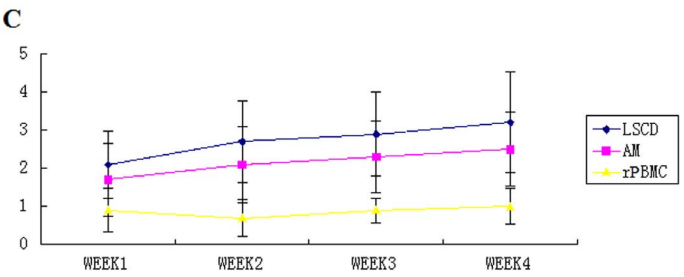

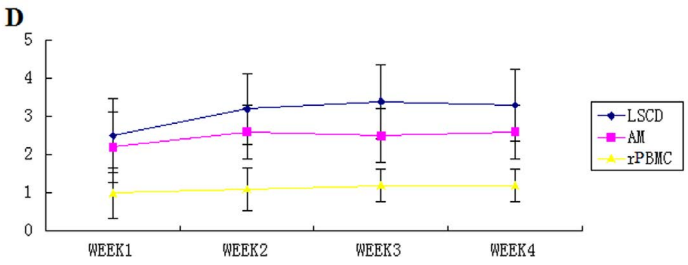

Figure 5. Statistical analysis of corneal transparency and Neovascularization condition

(A). Detailed corneal transparency scores of three groups of rabbits within four weeks. See supplement data figure-1 for full details.

(B). Detailed corneal neovascularization score of three groups of rabbits within four weeks. See supplement data figure-2 for full details.

(C). Changes in transparency at different time points around the linear graph

(D). Changes in Neovascularization at different time point around the linear graph.

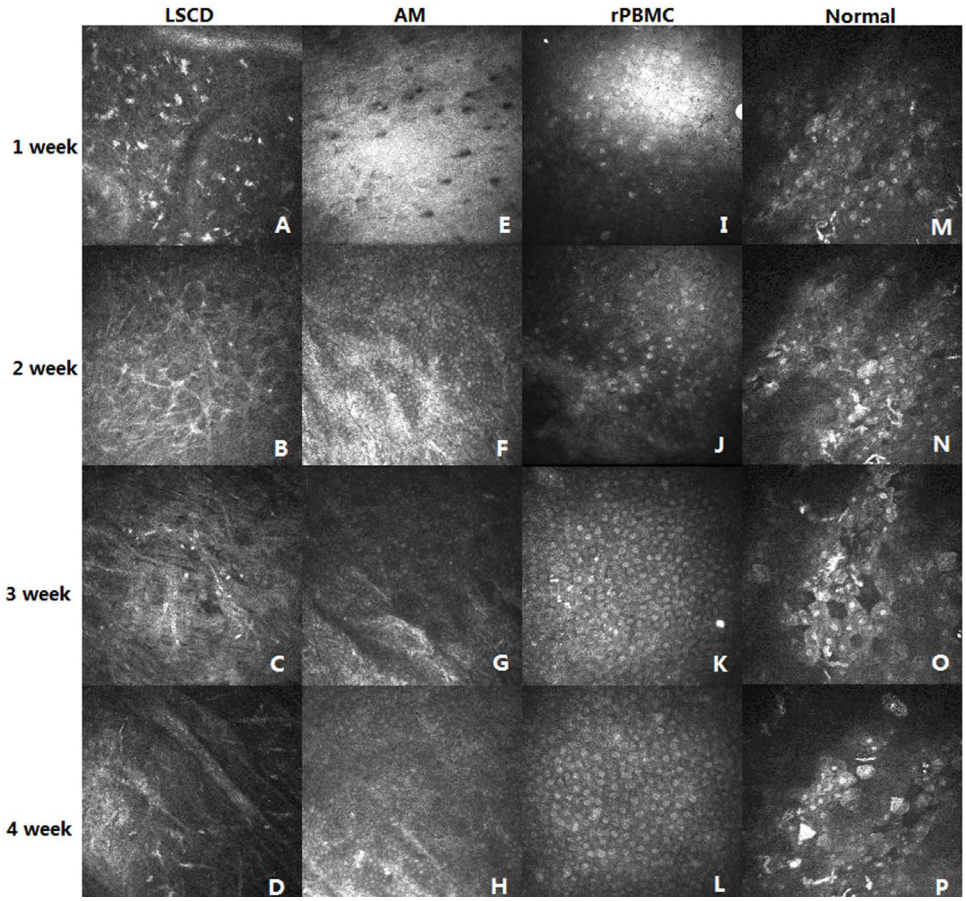

Figure 6. Confocal microscopy

(A)-(D). Changes in the LSCD group of epithelial cells under confocal microscopy within four weeks

(E)-(H). Changes in the AM group of epithelial cells under confocal microscopy within four weeks

(I)-(L). Changes in the rPBMC group of epithelial cells under confocal microscopy within four weeks

(M)-(P). Image of normal corneal epithelium under confocal microscopy

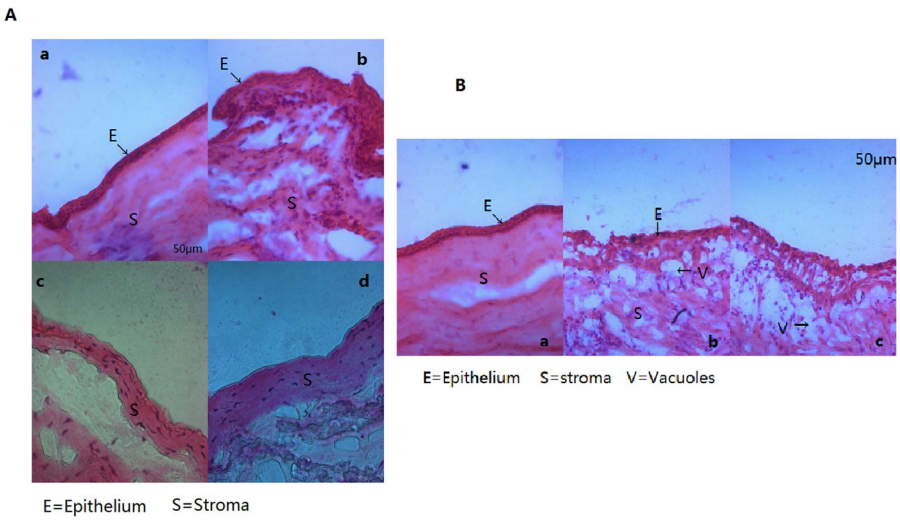

Figure 7. Histological Examination

(A). a. HE staining of normal corneal tissue(E=Epithelium, S=Stroma). b. HE staining of normal corneal limbal tissue. c. HE staining of corneal tissue after removal of corneal epithelium. d. HE staining of corneal tissue after removal of corneal epithelium.

(B). a. Four weeks after operation, HE staining of corneal tissue in rPBMC group (E=Epithelium, S=Stroma). b. Four weeks after operation, HE staining of corneal tissue in AM group (E=Epithelium, V=Vacuoles).

numerous cells in the AM group cornea were positive (Supplementary Figure 6(2)), indicating more frequent apoptosis. Normal cornea contained no detectable TUNEL+ cells (Supplementary Figure 6(3))

Dynamic changes of CM-DiI labeled rabbit PBMCs after transplantation

In addition to the changes in corneal epithelial cell marker expression and apoptosis, changes in rabbit autologous PBMC numbers were assess by CM-Dil staining. At postoperative 1W, numerous CM-DiI-labeled cells were observed in the rPBMC group. These numbers decreased with time post-surgery, and CM-DiI-labeled cells were no longer detectable at postoperative 4W (Supplementary Figures 4-6).

Discussion

Recent studies affirm that ESCs, iPSCs, and a variety of adult stem cells can be transdifferentiated into various triploblastic cells [32-41]. The application of stem cells for the prevention and treatment of human diseases has been also studied extensively, including for myocardial infarction, pancreatic disease, and liver disease [42-45]. Compared to other stem cells, PBMCs have several advantages, most importantly the potential for abundant and non-invasive acquisition from the

The model group receiving rabbit PBMC plus HAM transplantation exhibited significantly higher corneal transparency, lower neovascularization, more complete recovery of the corneal epithelium, and lower apoptotic rate than groups receiving no transplantation or HAMs alone. These results strongly suggest that autologous PBMCs can facilitate the recovery of severe ocular surface disorders caused by limbal stem cell deficiency. One possible mechanism is inhibition of inflammation, which could reduce progressive ocular damage and inhibit neovascularization by secreted angiogenic factors. In addition, stem/progenitor cells in PBMCs may have transdifferentiated into corneal epithelial cells within this favorable corneal microenvironment, thereby promoting recovery [26-29,30].

Confocal laser microscopy can specifically detect laser light reflection from the focal plane of living animal cornea, while reflected or scattered light outside the focal plane is blocked or filtered, yielding high-definition corneal images. Such dynamic in situ observation revealed that epithelial cells appeared earlier and expanded faster on corneal surfaces treated with rPBMCs.

Rabbit PBMCs do not express K3/K12 or β-1 integrin (supplementary Figure 3). Rather, K3/K12 is a specific marker for corneal epithelial cells, while β-1 integrin is expressed by epithelial stem/progenitor cells [38]. At 1W after cell transplantation, very few of K3/K12+ and β-1 integrin+ fluorescent cells were observed on the corneal surface of operative eyes in the rPBMC Group, but fluorescent immunopositive cell numbers increased with time such that the corneal surface was extensively covered by K3/K12+ andβ-1 integrin+ cells by W4. In contrast, few such cells were detected in AM and LSCD Groups, suggests more rapid and complete recovery of corneal epithelium in the rPBMC Group.

In contrast to this increase in K3/K12+ and β-1 integrin+ cells, the numbers of CM-DiI-labeled autologous PBMCs decreased with time, and no CM-DiI+ cells were detected by W4. One possible explanation for this disappearance is dilution of dye due to proliferation of the stem/progenitor cell fraction coupled with elimination of labeled terminal cells such as lymphocytes through apoptosis and removal by ocular tears. Due to this reduction in fluorescence, CM-DiI may not permit long-term tracing of PBMCs [46-47], so the use of alternative markers is required to assess PBMC fate in this model.

Declarations

Ethics approval and consent to participate

All animal experiments were approved by the Laboratory Animal Ethics Committee of Zhongshan Ophthalmic Center, Sun Yat-Sen University (Approval Number: 2013-060).

Consent for publication

All authors have approved the submission for publication.

Availability of data and materials

All data generated or analysed for this study are included in this published article.

Funding

This study was funded by the Science and Technology Projects of Guangdong Province, China (2017A030303013 and 2013B020400003), the Provincial.

Frontier and Key Technology Innovation Special Fund of Guangdong Province, China (2015B020227001), and the Science and Technology Program of Guangzhou, China (15570001).

Acknowledgements

Thanks to Pengxia Wan for the guidance of the operation.

Author Contribution

B. H. and Z. W.: Experimental design and manuscript preparation.

H. Z., M. Z., Q. L., and Y. X.: Corneal lesioning, Cell culture, Measurements, Statistical analysis and manuscript preparation.

M. Z. and M. H.: Pathological histology and immunofluorescence histological examination.

W. L., W. W., and Z. L.: Animal modeling and monitoring.

B. X., Y. L., and X. Z.: Image processing, Cell culture, and Amniotic membrane graft preparation.

Competing interest

All authors declare that they have no competing interest.

References

1. Zhang M and Huang B (2012) The multi-differentiation potential of peripheral blood mononuclear cells. *Stem Cell Res Ther* 3: 48-58. [Crossref]

2. Hassan HT, Zeller W, Stockschläder M, Krüger W, Hoffknecht MM, et al. (1996) Comparison between bone marrow and G-CSF-mobilized peripheral blood allografts undergoing clinical scale CD34+ cell selection. *Stem Cells* 14: 419-429. [Crossref]

3. Singh VK, Kalsan M, Kumar N, Saini A, Chandra R (2015) Induced pluripotent stem cells: applications in regenerative medicine, disease modeling, and drug discovery. Front Cell Dev Biol 2015; February 2; 3:2. [Crossref]

4. Yu J, Vodyanik MA, Smuga-Otto K, Antosiewicz-Bourget J, Frane JL, et al. (2007) Induced pluripotent stem cell lines derived from human somatic cells. *Science* 318: 1917-1920.

5. Liu Q, Guan L, Huang B, Li W, Su Q, et al. (2011) Adult peripheral blood mononuclear cells transdifferentiate in vitro and integrate into the retina in vivo. *Cell Biology International* 35: 631-638.

6. Zhang Y, Huang B (2012) Periphral blood cells: phenotypic deversity and potential clinical applications. *Stem Cell Rev* 8: 917-925. [Crossref]

7. Peng Y, Zhang Y, Huang B, Luo Y, Zhang M, et al. (2014) Survival and migration of pre-induced adult human peripheral blood mononuclear cells in retinal degeneration slow (rds) mice three months after subretinal transplantation. *Curr Stem Cell Res Ther* 9: 124-133. [Crossref]

8. Xian B, Zhang Y, Peng Y, Huang J, Li W, et al. (2016) Adult human peripheral blood mononuclear cells are capable of producing neurocyte or photoreceptor-like cells that survive in mouse eyes after pre-induction with neonatal retina. *Stem Cells Transl Med* 5: 1515-1524. [Crossref]

9. Pellegrini G, Rama P, Mavilio F, De Luca M. Epithelial stem cells in corneal regeneration and epidermal gene therapy. *J Pathol* 217: 217-228. [Crossref]

10. Lim P, Fuchsluger TA, Jurkunas UV (2009) Limbal stem cell deficiency and corneal neovascularization. *Semin Ophthalmol* 24: 139-148. [Crossref]

11. Ahmad S (2012) Concise review: limbal stem cell deficiency, dysfunction, and distress. *Stem Cells Transl Med* 1: 110-115. [Crossref]

12. Osei-Bempong C, Figueiredo FC, Lako M (2013) The limbal epithelium of the eye--a review of limbal stem cell biology, disease and treatment. *Bioessays* 35: 211-219. [Crossref]

13. Dua HS, Azuara-Blanco A (2002) Limbal stem cells of the corneal epithelium. *Surv Ophthalmol* 44: 415-425. [Crossref]

14. Tseng S (1989) Concept and application of limbal stem cells. *Eye (Lond)* 3: 141-157. [Crossref]

15. Rama P, Matuska S, Paganoni G, Spinelli A, De Luca M, et al. (2010) Limbal stem-cell therapy and long-term corneal regeneration. *N Engl J Med* 363: 147.

16. Wagoner MD (1997) Chemical injuries of the eye: current concepts in patho-physiology and therapy. *Surv Ophthalmol* 41: 275-313. [Crossref]

17. Zhu J, Zhang K, Sun Y (2013) Reconstruction of functional ocular surface by a cellular porcine cornea matrix scaffold and limbal stem cells derived from human embryonic stem cells. *Tissue Eng Part A* 19: 2412-2425. [Crossref]

18. Zhang H, Lin S, Zhang M (2017) Comparison of Two Rabbit Models with Deficiency of Corneal Epithelium and Limbal Stem Cells Established by Different Methods. *Tissue Eng Part C Methods*.

19. Cardoen L, Foets B (1999) Limbal transplantation after chemical injuries of the eye. *Bull Soc Belge Ophtalmol* 272: 105-110. [Crossref]

20. Muraine M, Salessy P, Watt L, Retout A, Brasseur G (2000) Limbal autograft transplantation, eight consecutive cases. *Journal Francais D' Ophtalmol* 23: 141-150. [Crossref]

21. Holland EJ (1996) Epithelial transplantation for the management of severe ocular surface disease. *Trans Am Ophthalmol Soc* 94: 677-743. [Crossref]

22. Reinhard T, Sundmacher R, Spelsberg H, Althaus C (1999) Homologous penetrating central limbo-keratoplasty (HPCLK) in bilateral limbal stem cell insufficiency. *Acta Ophthalmol Scand* 77: 663-667. [Crossref]

23. Kim JC, Tseng SC (1995) Transplantation of preserved human amniotic membrane for surface reconstruction in severely damaged rabbit corneas. *Cornea* 14: 473-484. [Crossref]

24. Malhotra C, Jain AK (2014) Human amniotic membrane transplantation: Different modalities of its use in ophthalmology. *World J Transplant* 4: 111-121. [Crossref]

25. Chugh JP, Jain P, Sen R (2015) Comparative analysis of fresh and dry preserved amniotic membrane transplantation in partial limbal stem cell deficiency. *Int Ophthalmol* 35: 347-355. [Crossref]

26. Sareen D, Saghizadeh M, Ornelas L (2014) Differentiation of human limbal-derived induced pluripotent stem cells into limbal-like epithelium. *Stem Cells Transl Med* 3: 1002-1012. [Crossref]

27. Nakatsu MN, González S, Mei H, Deng SX (2014) Human limbal mesenchymal cells support the growth of human corneal epithelial stem/progenitor cells. *Invest Ophthalmol Vis Sci* 55: 6953-6959. [Crossref]

28. Rohaina CM, Then KY, Ng AM (2014) Reconstruction of limbal stem cell deficient corneal surface with induced human bone marrow mesenchymal stem cells on amniotic membrane. *Transl Res* 163: 200-210. [Crossref]

29. Yang X, Moldovan NI, Zhao Q (2008) Reconstruction of damaged cornea by autologous transplantation of epidermal adult stem cells. *Mol Vis* 14: 1064-1070. [Crossref]

30. Meyer-Blazejewska EA, Call MK, Yamanaka O (2011) From hair to cornea: toward the therapeutic use of hair follicle-derived stem cells in the treatment of limbal stem cell deficiency. *Stem Cells* 29: 57-66. [Crossref]

31. Zhang W, Yang W, Liu X, Zhang L, Huang W, et al. Rapidly constructed scaffold-free embryonic stem cell sheets for ocular surface reconstruction. *Tissue Eng Part C Methods* 36: 286-292. [Crossref]

32. Wan P, Wang X, Ma P (2011) Cell delivery with fixed amniotic membrane reconstructs corneal epithelium in rabbits with limbal stem cell deficiency. *Invest Ophthalmol Vis Sci* 52: 724-730. [Crossref]

33. Zhang Y, Luo Y, Li K (2013) Pre-induced adult human peripheral blood mononuclear cells migrate widely into the degenerative retinas of rd1 mice. *Cytotherapy* 15: 1416-1425.

34. Guan L, Yu J, Zhong L (2011) Biological safety of human skin-derived stem cells after long-term in vitro culture. *J Tissue Eng Regen Med* 5: 97-103. [Crossref]

35. Huang B, Li K, Yu J (2013) Generation of human epidermis-derived mesenchymal stem cell-like pluripotent cells (hEMSCPCs). *Sci Rep* 3: 1933. [Crossref]

36. Wagers AJ (2012) The stem cell niche in regenerative medicine. *Cell Stem Cell* 10: 362-369. [Crossref]

37. Eisenberg LM, Eisenberg CA (2003) Stem cell plasticity, cell fusion, and transdifferentiation. *Birth Defects Res C Embryo Today* 69: 209-218. [Crossref]

38. Gao N, Wang Zh, Huang B (2007) Putative epidermal stem cell convert into corneal epithelium-like cell under corneal tissue in vitro. *Sci China C Life Sci* 50: 101-110. [Crossref]

39. Wang Z, Ge J, Chen J, Huang B (1999) Preliminary experimental study on commitment differentiation of embryonic stem cells induced by corneal limbal stroma in vitro. *Eye Science* 15: 195-198. [Crossref]

40. Tao J, Ge J, Huang B (2003) Preliminary study on induction of mouse embryonic stem cells into neural stem cells in vitro. *Chinese Journal of Pathophysiology* 19: 289-292.

41. Guan L, Yu J, Huang B (2010) In vitro differentiation of human skin-derived mesenchymal stem cells into lymphocytes: Possibility evaluation. *Journal of Clinical Rehabilitative Tissue Engineering Research* 14: 3601-3605.

42. Blazejewska EA, Schlötzer-Schrehardt U, Zenkel M (2009) Corneal limbal microenvironment can induce transdifferentiation of hair follicle stem cells into corneal epithelial-like cells. *Stem Cells* 27: 642-652. [Crossref]

43. Zhang J, Ho JC, Chan YC, Lian Q, Siu CW, et al. (2014) Overexpression of myocardin induces partial transdifferentiation of human-induced pluripotent stem cell-derived mesenchymal stem cells into cardiomyocytes. *Physiol Rep* 2: e00237. [Crossref]

44. Numasawa Y, Kimura T, Miyoshi S (2011) Treatment of human mesenchymal stem cells with angiotensin receptor blocker improved efficiency of cardiomyogenic transdifferentiation and improved cardiac function via angiogenesis. *Stem Cells* 29: 1405-1414. [Crossref]

45. Bouwens L (1998) Transdifferentiation versus stem cell hypothesis for the regeneration of islet beta-cells in the pancreas. *Microsc Res Tech* 43: 332-336. [Crossref]

46. Lue J, Lin G, Ning H, Xiong A, Lin CS et al. (2010) Transdifferentiation of adipose-derived stem cells into hepatocytes: a new approach. *Liver International* 30: 913-922.

47. Schormann W, Hammersen FJ, Brulport M (2008) Tracking of human cells in mice. *Histochem Cell Biol* 130: 329-338. [Crossref]

48. Chen X, Wang C, Feng Y (2009) Feasibility of CM-DiI as a tracer in bone marrow stem cell transplantation. *Journal of Clinical Rehabilitative Tissue Engineering Research* 13: 3611-3615.

49. Mathivanan I, Trepp C, Brunold C, Baerlocher G, Enzmann V (2015) Retinal differentiation of human bone marrow-derived stem cells by co-culture with retinal pigment epithelium in vitro. *Exp Cell Res* 333: 11-20. [Crossref]